# Synthesis and Solution Properties of Deferoxamine Amides

**PETER M. IHNAT,[1,2] JONATHAN L. VENNERSTROM,[1] DENNIS H. ROBINSON[1]**

[1] Department of Pharmaceutical Sciences, College of Pharmacy, University of Nebraska Medical Center, 986025 Nebraska Medical Center, Omaha, Nebraska 68198-6025

[2] Schering-Plough Research Institute; K-11-2-J5, 2000 Galloping Hill Road, Kenilworth, New Jersey 07033

*Received 26 August 1999; revised 3 July 2000; accepted 29 July 2000*

**ABSTRACT:** The poor membrane permeability and oral bioavailability of the iron chelating agent deferoxamine (DFO) mesylate result from the low octanol/water partition coefficient and high aqueous solubility. With the ultimate aim to improve biomembrane permeability while retaining the iron-binding ability of DFO, a series of more lipophilic amides were prepared by reacting the terminal primary amino group with fatty and aromatic acid chlorides or anhydrides. Octanol/water partition coefficients and equilibrium solubilities of these analogs in solvents, chosen to delineate physicochemical interactions, were determined as a function of temperature. Solid-state properties were evaluated by calorimetry. All DFO amide derivatives had higher melting points, indicating that derivatives formed strong intermolecular interactions in the solid phase. Formamidation of the primary amine of deferoxamine resulted in a 200-fold increase in the octanol/water partition coefficient and reduced aqueous solubility at least 2000-fold compared with the parent molecule. The partition coefficient increased and aqueous solubility decreased 2-fold with the addition of each methylene group in the homologous series of aliphatic amides. Solubilities of the derivatives in water-saturated octanol and hexane showed irregular profiles as a function of increasing aliphatic chain length that were attributed to intermolecular packing in the solid state. The temperature dependence of the partition coefficients was interpreted to indicate that interfacial transfer of the deferoxamine amides was, in part, affected by an apparent diminished ability to form energetically favorable interactions in the water-saturated organic phase.  J Pharm Sci 89:1525–1536, 2000
**Keywords:** deferoxamine; deferoxamine derivatives; iron chelators; partition coefficient; solubility; thermodynamics

## INTRODUCTION

Deferoxamine mesylate (DFO, Figure 1), the only Federal Drug Administration (FDA) approved drug used to remove toxic levels of iron from the systemic circulation, strongly complexes the ferric ion to form the hexadentate complex, ferrioxamine ($K_f = 10^{30}$), which is readily excreted through the kidneys.[1] Toxic levels of systemic iron result primarily from accidental or intentional overdose, chronic blood transfusions, or thalassemia, a genetically acquired anemia that causes ineffective erythropoiesis and is endemic to the Mediterranean regions. The World Health Organization has identified thalassemia as the most severe and widespread single locus genetic disease in the world. Patients suffering from systemic iron overload require chronic subcutaneous injections or infusions of up to 80–120 mg/kg (4–12g DFO/day) through an externalized central venous catheter to maintain a negative iron balance.[2,3] The poor lipophilicity of DFO results in absorption of only 15% of an orally administered

*Correspondence to:* P.M. Ihnat (Telephone: 908-740-2101; Fax: 908-740-2802; E-mail: peter.ihnat@spcorp.com)

Journal of Pharmaceutical Sciences, Vol. 89, 1525–1536 (2000)

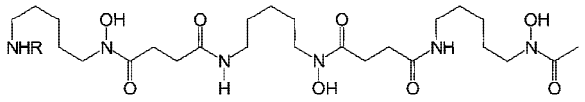

**Figure 1.** The structure of deferoxamine (R = H) and the deferoxamine derivatives. The R groups are listed in Table 2.

dose and inefficient mobilization of iron from tissues following parenteral administration in humans. Therefore, high dose infusions are required to mobilize iron from circulating transferrin and tissue stores.[2–4] Although high-dose DFO therapy is usually free of major side effects, auditory and visual abnormalities associated with neurotoxicity have been reported.[2,4] Because the once promising orally bioavailable iron chelator 1,2-dimethyl-3-hydroxypyrid-4-one has not advanced beyond clinical trials, DFO remains the only available drug for the treatment for systemic iron overload.[3] In addition to mobilizing systemic iron, DFO possesses moderate antimalarial activity and has been shown to block the iron-dependent generation of oxygen free radicals in the body.[5–7]

The primary amino group of DFO does not participate in the coordination of iron (III)(Figure 1) and contributes to the low lipophilicity of this iron chelator because it is protonated at physiological pH.[8] The overall hypothesis of this research is that modification of the amino group of DFO with lipophilic substituents should preserve the iron-binding ability, eliminate the charge, and theoretically improve biomembrane permeability allowing for a more efficient access to tissue iron stores. As a result, efficacy could be enhanced with decreased costs and improved patient compliance. The more lipophilic amide derivatives are also expected to be stable to hydrolysis within the gastrointestinal pH range 2–7.[9]

Generally, the addition of one methylene group into a molecular structure improves lipophilicity by a factor of 3 and removal of a charged group increases lipophilicity 100-fold.[10,11] As a result, acetylation of the primary amine of DFO could theoretically improve lipophilicity by a factor of 300. Incremental increases in the octanol/water partition coefficient of molecules as a result of structural modifications have been positively correlated with increases in biomembrane permeability, although the extent of improvement differs with each class of molecule.[12–16] Indeed, this approach has been partially successful for DFO as exemplified by the improved membrane permeability and antimalarial activity of the *N*-methylanthranilamide derivative of DFO.[6] In this work, we wished to extend these efforts by constructing a physicochemical database, starting with DFO amide derivatives, that may lead to the identification of an analog with optimal biomembrane permeability. The specific objectives were to identify and evaluate the physicochemical solution properties of DFO, synthesize a series of DFO amide derivatives that demonstrate a range of solution properties, determine their aqueous and organic solvent solubilities as well as octanol/water partition coefficients, and compare the properties with reported characteristics necessary for biomembrane permeability.

## MATERIALS AND METHODS

### Synthesis of Deferoxamine Derivatives

#### *Aliphatic and Aromatic Amides of Deferoxamine*

DFO (1 mmol) was dissolved in 10 mL of distilled $H_2O$ and the pH adjusted to 8–9 with 5 M KOH. An excess (6 mmol) of the appropriate acid chloride or anhydride was dissolved in 1–2 mL of $CHCl_3$ and added in a dropwise manner over a period of 30 min to the DFO solution at room temperature while maintaining the pH between 8 and 9. Reaction mixtures were extracted with $CHCl_3$ and dried with anhydrous $Na_2SO_4$. The $CHCl_3$ was removed *in vacuo,* and the oily residues of the tetracylated DFO intermediates were redissolved in 20 mL of MeOH, placed in an ice bath, and aerated with anhydrous ammonia gas that was bubbled through the solutions for 1 h to liberate the free hydroxamic acid functional groups. Following refrigeration for at least 12 h, the solid monoacylated deferoxamine derivatives were collected after vacuum evaporation. The off-white solids were recrystallized from absolute ethanol or *n*-propanol[17,18] (30–50% yields). The propyl, butyl, valeryl, caproyl, octanoyl, benzoyl, and phenylacetyl DFO derivatives were synthesized from the acid chloride, and the acetamide and succinamide derivatives were synthesized from the corresponding anhydrides.

#### *Acetamide Deferoxamine*

Anal. Calcd for $C_{27}H_{50}O_9N_6$: C, 53.8% H, 8.3% N, 14.0%. Found: C, 54.0%; H, 8.4%; N, 13.9%; mp 175.7 °C; $^1$H NMR: δ 1.20–1.53 (m, 18H), 1.79 (s, 3H), 1.98 (s, 3H), 2.28 (m, 4H), 2.59 (m, 4H), 3.00

(m, 6H), 3.48 (m, 6H), 7.81 (m, 3H), 9.68 (br s, 3H).

### *Propylamide Deferoxamine*

Anal. Calcd for $C_{28}H_{52}O_9N_6$: C, 54.5%; H, 8.4%; N, 13.6%. Found: C, 54.6%; H, 8.4%; N, 13.4%; mp 176.4 °C; $^1$H NMR: δ 1.00 (m 4H), 1.22–1.52 (m, 18H), 1.97 (s, 2H), 2.04 (m, 2H), 2.29 (m, 4H), 2.60 (m, 5H), 3.00 (m, 6H), 3.40 (m, 7H), 7.84 (m, 3H), 9.79 (br s, 2H).

### *Butylamide Deferoxamine*

Anal. Calcd for $C_{29}H_{54}O_9N_6$: C, 55.2%; H, 8.6%; N, 13.3%. Found: C, 55.2%; H, 8.6%; N, 13.2%; mp.177.9 °C; $^1$H NMR: δ 0.9 (m, 3H), 1.22–1.53 (m, 21H), 1.97 (s, 3H), 2.01 (m, 2H), 2.28 (m, 4H), 2.59 (m, 4H), 3.00 (m, 6H), 3.46 (m, 6H), 7.81 (m, 3H), 9.73 (br s, 2H).

### *Valeramide Deferoxamine*

Anal. Calcd for $C_{30}H_{56}O_9N_6$: C, 55.9%; H, 8.7%; N, 13.0%. Found: C, 56.0%; H, 8.6%; N, 13.0%; mp 180.4 °C; $^1$H NMR: δ 0.85 (m, 3H), 1.20–1.52 (m, 22H), 1.97 (s, 3H), 2.04 (m, 3H), 2.29 (m, 4H), 2.58 (m, 4H), 3.01 (m, 6H), 3.48 (m, 6H), 7.79 (m, 3H), 9.69 (br s, 3H).

### *Caproylamide Deferoxamine*

Anal. Calcd for $C_{31}H_{58}O_9N_6$: C, 56.5%; H, 8.8%; N, 12.8%; Found: C, 56.3%; H, 8.7%; N, 12.5%; mp 176.9 °C; $^1$H NMR: δ 0.85 (t, 3H), 1.18–1.52 (m, 25H), 1.97 (s, 3H), 2.03 (t, 2H), 2.29 (m, 5H), 2.57 (m, 4H), 3.01 (m, 6H), 3.45 (m, 6H), 7.80 (m, 3H), 9.72 (br s, 2H).

### *Octanoylamide Deferoxamine*

Anal. Calcd for $C_{33}H_{62}O_9N_6$: C, 57.7%; H, 9.0%; N, 12.2%, Found: C, 57.9%; H, 9.0%; N, 12.4%; mp 182.1 °C; $^1$H NMR: δ 0.86 (t, 3H), 1.23–1.49 (m, 28H), 1.97 (s, 3H), 2.02 (t, 2H), 2.26 (m, 4H), 2.57 (m, 4H), 2.98 (m, 6H), 3.45 (m, 7H), 7.80 (m, 3H), 9.72 (br s, 2H).

### *Benzoylamide Deferoxamine*

Anal. Calcd for $C_{32}H_{52}O_9N_6$: C, 57.8%; H, 7.8%; N, 12.7%; Found: C, 57.7%; H, 7.9%; N, 12.7%; mp 180.6 °C; $^1$H NMR: δ 1.25–1.54 (m, 18H), 1.98 (s, 3H), 2.28 (m, 4H), 2.60 (m, 4H), 3.02 (m, 4H), 3.26 (m, 3H), 3.47 (m, 5H), 7.60-7.80 (m, 7H), 8.20 (s, 1H), 9.60 (br s, 2H).

### *Phenylacetamide Deferoxamine*

Anal. Calcd for $C_{33}H_{54}O_9N_6$: C, 58.4%; H, 8.0%; N, 12.4%. Found: C, 58.2%; H, 7.9%; N, 12.2%; mp 174.5 °C; $^1$H NMR: δ 1.18–1.49 (m, 19H), 1.97 (s, 3H), 2.26 (m, 4H), 2.57 (m, 4H), 3.00 (m, 7H), 3.38–3.45 (m, 7H), 7.30–7.81 (m, 7H), 8.04 (s, 1H), 9.6 (br s, 2H).

### *Succinamide Deferoxamine*

Anal. Calcd for $C_{29}H_{51}O_{11}N_6$: C, 52.7%; H, 7.9%; N, 12.7%; Found: C, 52.9%; H, 7.9%; N, 12.5%;; mp 163 °C; $^1$H NMR: δ 1.18–1.54 (m, 19H), 1.99 (s, 3H), 2.31 (m, 8H), 2.40 (m, 4H), 3.03 (m, 6H), 3.47 (m, 7H), 7.86 (m, 3H), 9.70 (br s, 1H).

### *Formamide Deferoxamine*

DFO (1.5 mmol) and ethyl formate (20 mL) were added to a solution of 1% triethylamine in 30 mL of dimethylformamide (DMF), and the DFO suspension was refluxed for 15 h under nitrogen. The DFO dissolved during refluxing and the resulting formylated DFO derivative precipitated after subsequent cooling.[19] The off-white precipitate of DFO formamide was isolated by vacuum evaporation and filtration followed by re-crystallization from *n*-propanol (90% yield).

### *Formamide Deferoxamine*

Anal. Calcd for $C_{26}H_{48}O_9N_6$: C, 53.1%; H, 8.2%; N, 14.3%; Found: C, 53.3%; H, 8.2%; N, 14.3%; mp 157.6 °C; $^1$H NMR: δ 1.21–1.52 (m, 18H), 1.97 (s, 3H), 2.26 (m, 4H), 2.58 (m, 4H), 2.99-3.06 (m, 6H), 3.46 (m, 7H), 7.80 (m, 2H), 8.00 (s, 2H), 9.67 (br s, 2H).

### *Methylsulfonamide Deferoxamine*

Equimolar (1.5 mmol) of DFO and anhydrous ferric chloride were combined in distilled water (10 mL) and stirred for 15 min to form the deep-red, iron (III) chelate ferrioxamine. After the pH was adjusted to 8.5 with 5 M KOH, methylsulfonyl chloride (2 mL) dissolved in $CHCl_3$ (3 mL) was added in a dropwise manner into the stirred ferrioxamine solution over a period of 30 min while maintaining the pH at 8.5. The reaction solution was extracted with $CHCl_3$, and the volume of the aqueous phase was reduced ~50% *in vacuo*. A 10-fold molar excess of EDTA was added to the concentrated methylsulfonamide ferroxamine solution and, after adjusting the pH to 4.0, the solution was equilibrated for 48 h at 4 °C.[20] The more

water soluble iron(III)–EDTA complex remained dissolved, whereas the methylsulfonamide–DFO derivative precipitated and was collected by filtration. Recrystallization from ethanol yielded 20%.

### *Methylsulfonamide Deferoxamine*

Anal. Calcd for $C_{28}H_{50}O_{10}N_6S$: C, 48.9%; H, 7.8%; N, 13.2%; Found: C, 48.9%; H, 7.8%; N, 13.2%; mp 142.8 °C; $^1$H NMR: δ 1.23–1.50 (m, 18H), 1.97 (s, 3H), 2.27 (m, 5H), 2.58 (m, 4H), 2.86 (s, 4H), 3.00 (m, 4H), 3.46 (m, 8H), 7.81 (m, 2H), 9.67 (br s, 2H).

## Thermal Analysis

Differential scanning calorimetry (DSC; Shimadzu DSC-50) was used to determine the melting points ($T_m$) and heats of fusion ($\Delta H_f$) of the DFO amides. Approximately 0.8 to 1.2 mg of each DFO analog was sealed in an aluminum pan and heated at 10 °C/min under $N_2$ atmosphere (20 mL/min flow rate). Thermal profiles of the analogs revealed one corresponding endothermic peak. Temperature cycling experiments confirmed the absence of polymorphism. Melting points and heats of fusion were calculated using associated software.

## Spectrophotometric Analysis

A Shimadzu UV 160U double beam spectrophotometer was used to generate calibration curves of all DFO amides at 230 nm in 0.1 M NaOH and at 208 or 210 nm in water-saturated octanol. For both solvents, the concentration range was 5–55 μg/mL, and the mean absorbance of triplicate measurements were recorded.

## Octanol/Aqueous Distribution Coefficients

All glassware used in these experiments was rinsed with 0.1 M HCl and freshly distilled, deionized $H_2O$ to ensure the absence of glass-bound iron. Phosphate buffers of constant ionic strength (0.1), were prepared at pH 5.0, 7.4, and 8.0. The octanol and aqueous phases were mutually presaturated by vigorous stirring for at least 12 h.

Equal volumes (10 mL) of the aqueous DFO solutions and organic phases were combined in a glass-stoppered flask, placed in a temperature-controlled water-bath, and stirred for 24 h. After equilibration, the phases were separated by centrifugation at 1000 rpm for 15 min and DFO concentrations in both phases were determined spectrophotometrically (octanol λ = 210 nm, water λ = 220 nm).

The partition coefficients of the DFO derivatives were determined at 25 and 37 °C, and the distribution coefficients in phosphate buffer (pH 7.4, $I$ = 0.1) were determined at 25 °C. Analog concentrations in octanol were analyzed directly by spectrophotometry (λ = 210 nm), whereas the aqueous phase was diluted 4:1 with 0.5 N NaOH prior to spectrophotometric analysis (λ = 230 nm).

$$P = \frac{[A]_o}{[A]_w} \tag{1}$$

The intrinsic partition coefficient ($P$) was calculated from the ratio of the solute concentration in water-saturated octanol ($[A]_O$) and octanol-saturated water ($[A]_W$) at equilibrium. The thermodynamic partition coefficient ($P_x$), which is used to evaluate the thermodynamic parameters associated with solute partitioning, was calculated from the ratio of the solute mole fraction concentrations in water saturated octanol ($X_{2^o}$) and octanol saturated water ($X_{2^w}$):

$$P_x = \frac{X_2^o}{X_2^w} \tag{2}$$

The free energy of solute partitioning between water and octanol ($\Delta G_{tr}$, kJ/mol) was calculated from the thermodynamic partition coefficient using eq. 3:

$$\Delta G_{tr} = 2.303\, R\, T \log P_x \tag{3}$$

where $R$ is the universal gas constant (8.314 J/mol K).

## Aqueous Solubilities

The solubilities of the DFO derivatives were evaluated in triplicate in freshly distilled deionized water, distilled water acidified with 0.01 M HCl to pH 4–5, and phosphate buffer (pH 7.4, $I$ = 0.1) using glassware presoaked in 0.1 M HCI and rinsed in deionized water. Vials, containing an excess of each DFO analog, were placed in a temperature-controlled environment and agitated for at least 4 days while being periodically monitored

**Table 1.** Octanol/Water and Octanol/Buffer Distribution Coefficients of Deferoxamine[a]

| Temperature, °C | Solvent | $P$[b] | $P_x$[c] | $\Delta G$ (kJ/mol)[d] |
|---|---|---|---|---|
| 15 | water | 0.0013 ± 0.0003 | 0.011 ± 0.002 | 10.83 ± 0.44 |
| 25 | water | 0.0022 ± 0.0001 | 0.019 ± 0.001 | 9.82 ± 0.52 |
| 37 | water | 0.0025 ± 0.0002 | 0.022 ± 0.002 | 9.84 ± 0.89 |
| 25 | buffer pH 5.0[e] | 0.0037 ± 0.0007 | — | — |
| 25 | buffer pH 7.4[e] | 0.0141 ± 0.0020 | — | — |
| 25 | buffer pH 8.0[e] | 0.0084 ± 0.0004 | — | — |

[a] $n = 3$.
[b] Calculated using eq 1.
[c] Calculated using eq 2.
[d] Calculated using eq 3.
[e] Phosphate buffer, ionic strength = 0.1.

for saturation. At equilibrium, samples were filtered and analyzed as already described.

### Octanol and Hexane Solubilities

The solubilities of each DFO amide in water-saturated octanol and in *n*-hexane were determined at 25 °C by the procedure previously described. After saturation was confirmed, the suspensions were centrifuged at 7000 rpm for 20 min, and the concentrations of the DFO analogs in the clear octanol fraction were analyzed spectrophotometrically ($\lambda$ = 210 nm). The suspensions in hexane were centrifuged at 2000 rpm for 20 min, and the supernatant was evaporated in a vacuum oven at ambient temperature. The residue was dissolved in 0.1 N NaOH and analyzed spectrophotometrically ($\lambda$ = 230 nm).

## RESULTS AND DISCUSSION

The hydrophilic nature of DFO (Figure 1) is characterized by the low distribution coefficients (Table 1) and high aqueous solubilities (>38.0 ± 4.4 g/100 mL) in the pH range of 4.2 to 8.0 at 25 °C.[21] Generally, the octanol/water distribution coefficients increased with temperature and were ~2–4-fold lower than the octanol/buffer distribution coefficients determined at 25 °C (Table 1). Therefore, because DFO is a relatively large, flexible molecule with polar hydroxamic acid and amide groups, cosolutes will contribute to the array of complex solvent–solute and solute–solute interactions in solution and at the organic/aqueous interface. For ionizable solutes, the interfacial distribution between an aqueous and organic phase is pH dependent.[12,22] The intrinsic partition coefficient refers to the ratio of the concentrations of the unionized, monomeric solute in both phases whereas the distribution coefficient refers to the ratio of the multiple ionic species partitioning between both phases.[22] The profile of the pH-dependent distribution of the ionic species of DFO was determined using previously reported p*K*a values and equations describing the relevant ionic equilibria in solution (Figure 2).[8,21]

The lower dielectric constant of water-saturated octanol (8.58) relative to octanol-saturated water (76.6) indicates that octanol cannot satisfy the electrical requirements of charged moieties as well as water.[12] In phosphate buffer (pH 5.0, 7.4, and 8.0), ionic species of DFO are free to form coulombic and hydrogen-bonding interactions with water or cosolutes. The increase in the distribution coefficient in buffer relative to water may result from ion-pair formation at the organic interface with the mesylate or phosphate counterions that partially neutralize the charges and re-

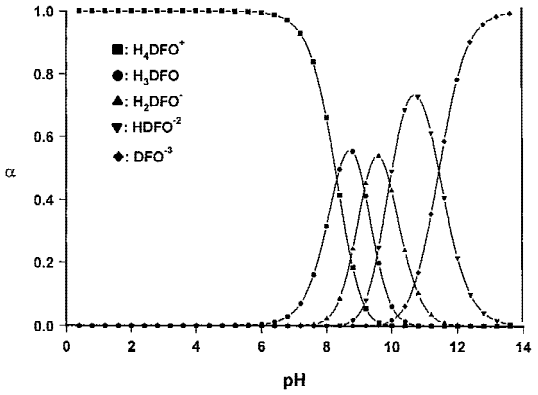


**Figure 2.** The distribution profile of deferoxamine species in solution as a function of pH. The symbol α refers to the fraction of each species.

duce resistance to incorporation into the octanol phase (Table 1).[23] At pH 7.4 and 8.0, the opposite charges of the zwitterionic form of DFO ($H_3$DFO, Figure 2) may be neutralized due to mutual attraction facilitated by conformational flexibility. This neutralization may facilitate accommodation of DFO into the lower dielectric environment of the organic phase.[23]

The thermodynamics of the partitioning of DFO was investigated in the octanol/water system to reduce additional intermolecular interactions that occur in presence of buffer ions (Table 1). The equation generated by linear regression of the van't Hoff plot was ($r = 0.931$, $n = 3$):

$$\log P_x = (1247.229 \pm 490.614)\frac{1}{T} + 2.401 \pm 1.646 \quad (4)$$

The positive free energy ($\Delta G$) values, calculated from the thermodynamic partition coefficients with eq. 3, indicate that interfacial transfer of DFO is energetically unfavorable. The endothermic enthalpy ($\Delta H = 23.88 \pm 9.39$ kJ/mol) signifies that the system must absorb energy to accommodate DFO into the hydrated organic phase.

Based on the number of hydrogen-bonding groups, the empirical hydrogen-bonding potential of DFO was determined to be 14.[24] Consequently, solute–solvent hydrogen bonding should contribute to the solubility of DFO in both water and octanol, and the energy required to disrupt hydrogen bonds between water and DFO should be offset by the energy gained from hydrogen-bond formation within water-saturated octanol and reflected in a lower enthalpy of partitioning. However, spectroscopic evidence in aqueous solution indicates that an intramolecular hydrogen bond is formed between the hydroxamic acid proton and adjacent carbonyl group, in lower molecular weight hydroxamic acids.[25,26] Because of the proximity of the carbonyl to the hydroxamic proton, the hydrogen bond may be too stable to reform in the water-saturated organic. Therefore, it appears that attractive forces between water and the charged amino group of DFO are more likely than hydrogen bonding to be responsible for the high aqueous solubility and low partition coefficients. Elimination of the charged amino group through derivatization should improve the lipophilicity and may enhance biomembrane permeability.[11,14]

The melting points and related thermal properties for the DFO derivatives are summarized in Table 2. Formamidation of the primary amino group of DFO increased the octanol/water partition coefficient >200-fold, and the octanol/buffer distribution coefficient 44-fold at 25 °C (Table 3). Addition of methyl or methylene groups further increased the partition coefficients in ~2-fold increments up to the butylamide ($COC_3H_7$) derivative. There was an abrupt 2.9-fold increase in partitioning between the butylamide and valeramide ($COC_4H_9$) DFO amides, after which no significant

**Table 2.** Molecular Weights and Thermal Properties of the Deferoxamine Derivatives

| Name | Derivative (R)[a] | MW | Melting Point (°C) | $\Delta H_f$ (kJ/mol)[c] | $\Delta S_f$ (kJ/mol K)[d] |
|---|---|---|---|---|---|
| deferoxamine[a] | DFO[a] | 563 | 137.9[b] | 105.3 | 0.26 |
| formamide- | COH | 588 | 157.6 | 92.93 | 0.22 |
| acetamide- | $COCH_3$ | 602 | 175.7 | 118.4 | 0.26 |
| propylamide- | $COC_2H_5$ | 616 | 176.4 | 116.9 | 0.26 |
| butylamide- | $COC_3H_7$ | 630 | 177.9 | 111.4 | 0.25 |
| valerylamide- | $COC_4H_9$ | 644 | 180.4 | 123.1 | 0.27 |
| caproylamide- | $COC_5H_{11}$ | 658 | 176.9 | 119.2 | 0.26 |
| octanoylamide- | $COC_7H_{15}$ | 686 | 182.1 | 130.7 | 0.29 |
| benzoylamide- | $COC_6H_5$ | 664 | 180.6 | 107.0 | 0.24 |
| phenylacetamide- | $COCH_2C_6H_5$ | 678 | 174.5 | 119.0 | 0.27 |
| succinamide- | $CO(CH_2)_2COOH$ | 660 | 163.0 | 101.0 | 0.24 |
| methylsulfonamide- | $SO_2CH_3$ | 638 | 142.8 | 117.8 | 0.28 |

[a] Figure 1.
[b] Deferoxamine mesylate.
[c] Heat of fusion.
[d] Entropy of fusion; $\Delta S_f = \Delta H_f/T_m$; 0.26 ± 0.02 (kJ/mol K).

**Table 3.** Distribution Coefficients of the Deferoxamine Derivatives

| | Octanol/Water (P)[b] | | Octanol/Buffer ($P_d$)[c] |
|---|---|---|---|
| Derivative (R)[a] | $T$ = 25 °C | $T$ = 37 °C | $T$ = 25 °C |
| COH | 0.47 ± 0.10 | 0.80 ± 0.06 | 0.62 ± 0.05 |
| $COCH_3$ | 0.93 ± 0.15 | 1.27 ± 0.08 | 1.45 ± 0.21 |
| $COC_2H_5$ | 1.48 ± 0.36 | 1.81 ± 0.09 | 1.57 ± 0.05 |
| $COC_3H_7$ | 2.61 ± 0.71 | 4.11 ± 0.36 | 4.56 ± 0.53 |
| $COC_4H_9$ | 7.61 ± 1.16 | 11.2 ± 0.53 | 7.65 ± 0.54 |
| $COC_5H_{11}$ | 8.30 ± 0.71 | 26.7 ± 3.47 | 12.5 ± 2.10 |
| $COC_7H_{15}$ | 8.70 ± 2.17 | 44.9 ± 10.7 | 12.3 ± 0.80 |
| $COC_6H_5$ | 1.99 ± 0.59 | 7.31 ± 1.06 | 3.34 ± 0.17 |
| $COCH_2C_6H_5$ | 1.67 ± 0.41 | 7.95 ± 1.69 | 1.79 ± 0.27 |
| $CO(CH_2)_2COOH$ | 0.31 ± 0.03 | 0.30 ± 0.03 | 0.02 ± 0.003 |
| $SO_2CH_3$ | 0.17 ± 0.04 | 0.44 ± 0.03 | 0.43 ± 0.11 |

[a] $n$ = 3.
[b] Intrinsic partition coefficient.
[c] Phosphate buffer, pH 7.4; ionic strength = 0.1.

increase in partition coefficient was observed (Table 3). Similarly, the octanol/buffer distribution coefficient increased 2 -fold with each addition of methyl or methylene group through caproylamide DFO ($COC_5H_{11}$). Commencing with valeramide DFO ($COC_4H_9$), the partition coefficients of the methylsulfonic ($SO_2CH_3$), aromatic ($COC_6H_5$, $COCH_2C_6H_5$), and longer-chain aliphatic derivatives were more sensitive to temperature than the short-chain aliphatic and succinamide ($CO(CH_2)_2COOH$) derivatives (Table 3). The correlation between the distribution and partition coefficients of all analogs except succinamide DFO ($r$ = 0.985), related by the fraction of ionized species in solution at pH 7.4, shows that the p$K$ values for the analogs are similar.[21,22]

The aqueous solubilities of the DFO analogs in phosphate buffer, pH 7.4, and distilled water are summarized in Table 4. The intrinsic solubility ($S_o$) or saturation solubility of the un-ionized species was obtained in acidified, distilled water to ensure that the solution pH was <8.5 or p$K_1$ of the first hydroxamic acid group.[8,17] Formamidation of the primary amino group of DFO reduced aqueous solubility at least 2000-fold. Additional methylene groups further reduced aqueous solubility

**Table 4.** Solubilities (μM) of the Deferoxamine Derivatives at 25 °C[a]

| R | $S_{PB}$[b] | $S_O$[c] | $S_W$[d] | $n$-Octanol[e] | $n$-Hexane |
|---|---|---|---|---|---|
| COH | 179 ± 1.9 | 201 ± 2.0 | 255 ± 14 | 81.6 ± 5.1 | 0.32 ± 0.15 |
| $COCH_3$ | 26.6 ± 1.7 | 48.2 ± 8.3 | 78.1 ± 5.0 | 73.1 ± 8.3 | 1.09 ± 0.10 |
| $COC_2H_5$ | 27.6 ± 1.6 | 29.2 ± 4.9 | 50.3 ± 5.0 | 56.8 ± 6.5 | 1.34 ± 0.60 |
| $COC_3H_7$ | 17.5 ± 1.6 | 15.9 ± 4.8 | 22.2 ± 1.6 | 44.4 ± 3.2 | 1.98 ± 0.52 |
| $COC_4H_9$ | 6.21 ± 1.5 | 7.76 ± 3.1 | 9.12 ± 1.5 | 59.0 ± 3.1 | 1.74 ± 0.04 |
| $COC_5H_{11}$ | 4.56 ± 1.5 | 7.60 ± 3.0 | 7.76 ± 1.6 | 86.6 ± 4.6 | 2.30 ± 0.34 |
| $COC_7H_{15}$ | 4.37 ± 1.4 | 5.83 ± 2.9 | 7.29 ± 2.9 | 65.6 ± 4.4 | 1.79 ± 0.42 |
| $COC_6H_5$ | 7.53 ± 1.5 | 12.1 ± 3.0 | 13.6 ± 4.5 | 33.1 ± 6.0 | 1.54 ± 0.65 |
| $COCH_2C_6H_5$ | 7.37 ± 1.5 | 13.3 ± 1.5 | 11.8 ± 3.0 | 28.0 ± 1.5 | 1.92 ± 0.39 |
| $CO(CH_2)_2COOH$ | <9000 | 147 ± 13 | 253 ± 18 | 48.5 ± 1.5 | 0.44 ± 0.10 |
| $SO_2CH_3$ | 113 ± 4.7 | 143 ± 4.7 | 176 ± 13 | 45.5 ± 1.6 | 0.99 ± 0.35 |

[a] $n$ = 3.
[b] Solubility in phosphate buffer, pH 7.4; ionic strength = 0.1.
[c] Intrinsic solubility.
[d] Solubility in unbuffered, distilled water.
[e] Water-saturated octanol.

in ~2-fold increments (Table 4). As expected, there was an inverse relationship between partitioning and intrinsic aqueous solubility for all 11 derivatives, but this correlation was most significant for the aliphatic homologs.[21] Although the first hydroxamic group was ~7% ionized at pH 7.4, the solubilities of the DFO analogs in phosphate buffer were comparable with their intrinsic aqueous solubilities (Table 4). Conversely, the analogs were most soluble in distilled water (5% ionized, mean pH 7.3 ±0.7) due to partial ionization in the absence of additional cosolute effects.

The solubilities of the DFO analogs were also evaluated in water-saturated octanol and *n*-hexane (Table 4). van der Waals interactions acted to dissolve the DFO analogs in hexane, whereas a combination of van der Waals forces and hydrogen bonding facilitated solubility in water-saturated octanol.[12,13] All derivatives were more soluble in water-saturated octanol than water or hexane because of intermolecular solute–solvent interactions with both polar and nonpolar regions (Table 4, Figure 3).[13] However, (at 25 °C), the solubilities of the aliphatic amides in hydrated octanol decreased by a factor of 1.23 ± 0.10 with each additional carbon atom up to butylamide DFO, after which there was an irregular solubility relationship. The abrupt upward trend in the octanol solubility profile of the aliphatic DFO homologs may represent the point where the aliphatic chain exerted more influence on solubility than the parent molecule (Figure 3). Conversely, the solubilities of the DFO analogs in hexane increased in an irregular pattern with each additional carbon atom (Table 4, Figure 3). Solubility in hexane was lower than in water and water-saturated octanol and relatively insensitive to incremental addition of carbon atoms (Figure 3).

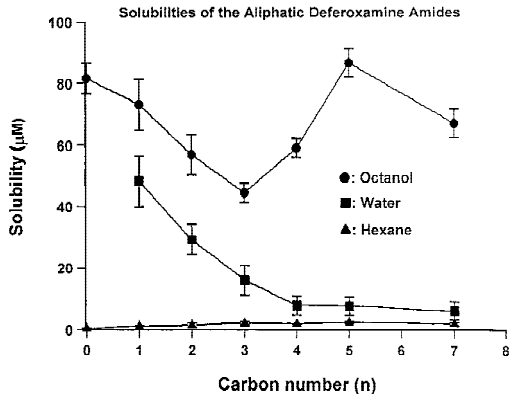


**Figure 3.** Comparison of water-saturated octanol, water, and *n*-hexane solubilities of the aliphatic deferoxamine analogs ($T$ = 25 °C).

Saturated aliphatic homologs of alkoxy, hydroxy, and amino benzoates also exhibited irregular patterns of solubility. These irregularities may be attributed to the structure-dependent crystal lattice energies in the solid state and were previously reported in homologs of 4 to 6 carbon atom chain lengths.[15,27,28] The melting points and heats of fusion of the aliphatic DFO homologs also increased irregularly with increasing carbon number (Table 2). The irregular solubility patterns and thermal properties may result from discrete differences in packing efficiency in the solid state, intramolecular degrees of freedom, and solvent cavity accommodation of the solute as dictated by carbon chain length.[15,28]

Except for formamide (COH), succinamide ($CO(CH_2)_2COOH$), and methylsulfonamide DFO ($SO_2CH_3$), the melting points of the remaining analogs were within 10 °C. The compounds with the highest solubilities in aqueous and octanol solution also had the lowest melting points (Tables 2 and 4). The relatively more bulky groups probably formed weaker intermolecular packing interactions that improved the escaping tendency from the solid phase.[23,28]

For the aliphatic DFO amide analogs, the semilogarithmic correlation between the hexane solubilities and the melting points ($r$ = 0.934, $n$ = 7) indicated that the disruption of the crystal lattice, and not solvent–solute van der Waals interactions, dominated the solution processes in hexane.[15] Regardless of modification, the entropies of fusion for all the DFO analogs were ~0.26 ± 0.02 kJ/mol K (Table 2). Therefore, in the solid state, substituents affected the attractive and repulsive forces, reflected in the enthalpy of fusion, more than the conformational degrees of freedom. The long aliphatic chains may stack to maximize contacts and despite being bulky, the aromatic derivatives may have formed π bonds with adjacent conjugated rings.[27,28]

The octanol/water partition coefficient of the DFO analogs may be calculated by the ratio of the analog solubility in octanol to water.[29] The correlation between the experimental octanol/water partition coefficient and the solubility ratio at 25 °C (Table 5) was:

$$\log P = 1.033 \pm 0.058 \log SR - 0.224 \pm 0.080 \quad (5)$$

where $n$ = 11 and $r$ = 0.986. Omitting the suc-

**Table 5.** Solubility Ratios of the Deferoxamine Derivatives

| R | SR[a] | SR[b] |
|---|---|---|
| COH | 0.41 | 0.54 |
| $COCH_3$ | 1.52 | 2.56 |
| $COC_2H_5$ | 1.94 | 1.65 |
| $COC_3H_7$ | 2.80 | 2.17 |
| $COC_4H_9$ | 7.60 | 8.00 |
| $COC_5H_{11}$ | 8.62 | 13.0 |
| $COC_7H_{15}$ | 11.0 | 9.00 |
| $COC_6H_5$ | 2.75 | 4.00 |
| $COCH_2C_6H_5$ | 2.11 | 4.20 |
| $CO(CH_2)_2COOH$ | 0.33 | — |
| $SO_2CH_3$ | 0.32 | 0.53 |

[a] Octanol solubility/intrinsic solubility ($S_0$) (data from Table 4).
[b] Octanol solubility/phosphate buffer solubility ($S_{PB}$) (data from Table 4).

cinamide derivative ($CO(CH_2)_2COOH$) from the regression due to a pH-dependent increase in aqueous solubility at pH 7.4, the relationship between the octanol/buffer distribution coefficient and solubility ratio at 25 °C was:

$$\log P = 0.989 \pm 0.141 \log SR - 0.064 \pm 0.210 \quad (6)$$

where $n = 10$ and $r = 0.927$. Using the solubility ratio to estimate the partition coefficient was valid because the solubilities of the DFO analogs in both solvents were < 0.01 M.[29] Because the solubility ratios were in excellent agreement with the partition coefficients, the increase in partitioning between formamide DFO (COH) and butylamide DFO ($COC_3H_7$) was related to a more rapid decline in aqueous solubility relative to solubility in water-saturated octanol with additional carbon atoms. The increase in partitioning between butylamide DFO ($COC_3H_7$) and valeramide DFO ($COC_4H_9$) may correspond to the point where the alkyl chain primarily influences solubility in water-saturated octanol while aqueous solubility continues to decline (Figure 3).

The free energy of partitioning of the DFO analogs between water and octanol ($\Delta G_{tr}$, kJ/mol) was calculated from the thermodynamic partition coefficient ($P_x$; eq. 3). The free energy of partitioning is comprised of the enthalpy ($\Delta H_{tr}$) and entropy ($\Delta S_{tr}$):

$$\Delta G_{tr} = \Delta H_{tr} - T\Delta S_{tr} \quad (7)$$

The enthalpy of partitioning represents the affinity of the solute for the solvent phase as a function of the solute–solvent and solvent–solvent interactions. The magnitude of the entropy of partitioning is affected by the conformation of the solute in the solvent and the conformational relationship between the solute and the solvent.[23] Assuming linearity in the Van't Hoff relationship between 25 and 37 °C, the enthalpy of partitioning may be calculated when the thermodynamic partition coefficients at two temperatures, $P_{x2}$ and $P_{x1}$, are known:

$$\log\left(\frac{P_{x2}}{P_{x1}}\right) = \left(\frac{\Delta H_{tr}}{2.303\ R}\right)\left(\frac{T_2 - T_1}{T_2 T_1}\right) \quad (8)$$

Although the intercepts of the Van't Hoff relationship were not available, the entropy of partitioning at a temperature between 25 and 37 °C may be estimated using eq. 7.[22]

The octanol/water partition coefficients of the DFO analogs were determined at 25 and 37 °C (Tables 3 and 6). The free energies of partitioning were negative and decreased with increasing temperature. The enthalpies of partitioning were positive for all compounds except succinamide DFO ($CO(CH_2)_2COOH$). Similar to smaller molecular weight hydroxamic acids and DFO, the analogs probably form an intramolecular hydrogen bond between the hydroxamic proton and adjacent carbonyl. This bond may diminish their ability to hydrogen bond within polar regions of the water-saturated octanol. Moreover, the energy required to perturb the "structure" of water-saturated octanol, by incorporation of the solute, may also contribute to the positive enthalpy of partitioning.[13] Because the enthalpies of partitioning were positive for the analogs, except succinamide DFO ($CO(CH_2)_2COOH$), a significant entropic contribution to partitioning may have helped to drive the reaction forward. The undissociated carboxylic acid group of succinamide DFO ($CO(CH_2)_2COOH$) may have formed a hydrogen bond within the water-saturated octanol resulting in the negative enthalpy of partitioning.

In summary, these results demonstrate that conversion of the protonated amino group of DFO to a variety of amides markedly decreased aqueous solubility and substantially increased lipophilicity relative to the parent molecule. The observed trends in the change in aqueous solubilities and partition coefficients for these analogs were consistent with those expected from incre-

**Table 6.** Thermodynamic Parameters of the Partitioning of the Deferoxamine Analogs

| R | $\Delta G$ (kJ/mol)[a] 25 °C | $\Delta G$ (kJ/mol)[a] 37 °C | $\Delta H$ (kJ/mol)[b] | $\Delta S$ (kJ/mol K)[c] |
|---|---|---|---|---|
| COH | –3.49 ± 0.71 | –5.03 ± 0.34 | 34.6 ± 7.40 | 0.13 ± 0.03 |
| $COCH_3$ | –5.20 ± 0.82 | –6.20 ± 0.39 | 19.7 ± 3.30 | 0.08 ± 0.01 |
| $COC_2H_5$ | –6.37 ± 0.88 | –7.15 ± 0.49 | 12.8 ± 2.00 | 0.06 ± 0.01 |
| $COC_3H_7$ | –7.75 ± 1.91 | –9.21 ± 0.88 | 28.7 ± 7.60 | 0.12 ± 0.03 |
| $COC_4H_9$ | –10.5 ± 1.30 | –11.8 ± 0.60 | 21.9 ± 2.90 | 0.11 ± 0.01 |
| $COC_5H_{11}$ | –10.6 ± 0.60 | –14.1 ± 1.90 | 74.7 ± 10.1 | 0.29 ± 0.03 |
| $COC_7H_{15}$ | –10.5 ± 2.00 | –15.4 ± 3.60 | 110 ± 34.0 | 0.41 ± 0.11 |
| $COC_6H_5$ | –6.76 ± 1.33 | –10.7 ± 1.60 | 91.5 ± 22.3 | 0.33 ± 0.08 |
| $COCH_2C_6H_5$ | –6.47 ± 1.29 | –11.1 ± 2.10 | 108 ± 29.3 | 0.38 ± 0.10 |
| $CO(CH_2)_2COOH$ | –2.46 ± 0.34 | –2.45 ± 0.24 | –2.66 ± 0.45 | $-0.001 \pm 10^{-4}$ |
| $SO_2CH_3$ | –1.21 ± 0.28 | –3.50 ± 0.21 | 55.6 ± 13.3 | 0.19 ± 0.05 |

[a] Calculated using eq. 3.
[b] Calculated using eq. 8.
[c] Calculated using eq. 7.

mental addition of carbon atoms. However, aqueous solubilities decreased more than expected, whereas lipophilicities did not increase to the degree expected. Also, the aliphatic amide DFO derivatives were relatively insoluble in the water-saturated octanol and hexane, indicating that the solid state was preferred to solution. Indeed, aliphatic and aromatic modifications, through intermolecular packing in the solid state, increased the melting points compared with DFO. This result is contrary to previous work with homologous series in which systematic declines in melting points as a function of increasing chain lengths or aromatic substituents were observed.[15,28,30]

Early studies of biomembrane permeability often concluded that the principal driving force was the gain in entropy resulting from the randomization of water molecules, surrounding a lipophilic solute (hydrophobic effect), on incorporation into the organic phase. These studies commonly used a saturated alkane/water partition coefficient as a reference system.[14,24] A number of studies have also shown that solutes that possess a strong ability to hydrogen bond in aqueous solution may not readily diffuse due to a high desolvation energy at the membrane interface.[31] Because the octanol/water system has been adopted as the reference for screening solutes for permeability potential, excellent correlations have been established between passive membrane diffusion and the partition coefficient for a variety of molecules. Hydrated octanol possesses polar and apolar localized environments similar to the interior of biomembranes.[13] Hence, a substituent decreases biomembrane permeability if it establishes attractive forces between the solute and water and increases membrane permeability if it enhances attractive forces between the solute and membrane. The solute must possess the ability to diffuse across the aqueous boundary layer adjacent to the membrane yet retain the capacity to form energetically favorable interactions in the membrane interior. Ideal modifications that facilitate passive transmembrane diffusion must alter physicochemical properties of a molecule by balancing energetically favorable solute–solvent interactions in both aqueous and organic phases with the entropic contribution.[14]

The permeabilities of selected deferoxamine derivatives were evaluated in preliminary experiments using the Caco-2 model. Approximately 1–1.6% of the acetamide ($COCH_3$) and propylamide ($COC_2H_5$) amides had permeated after 4 h. Also, the benzoylamide ($COC_6H_5$) and methylsulfonamide ($SO_2CH_3$) accumulations in the receiver compartments of the Transwell© plates were 1.7 and 2.2%, respectively, of the donor concentrations after 4 h. By comparison, ~0.05% DFO had permeated after 4 h. It remains to be seen whether the water-soluble formamide (COH) and succinamide ($CO(CH_2)_2COOH$) DFO analogs exhibit improved membrane permeabilities because their partition coefficients were ~50-fold higher than DFO and the octanol solubilities were comparable to the solubilities of the aliphatic and aromatic analogs. Therefore, the conclusions derived from

the physicochemical solution properties, regarding the biomembrane permeabilities of the DFO amides, are supported by these preliminary Caco-2 experiments.[21]

The transcellular permeability constant is directly proportional to the diffusion coefficient through the membrane and the diffusion coefficient is inversely proportional to the molecular size (conformation) or approximately (molecular weight)$^{1/3}$. Therefore, the molecular weight of the derivatives does affect passive transcellular absorption. However, because the molecular weights between the smallest and largest deferoxamine amides differed by only 17%, molecular weight differences are not likely to affect passive diffusion compared with other factors such as partition coefficient, aqueous solubility and molecular size (conformation).[24]

Although the charge of the primary amino group was eliminated and the analogs possessed improved lipophilicity, they also demonstrated weak solvent–solute interactions, which suggested that passive, transmembrane diffusion would be difficult. Nevertheless, as demonstrated by the parabolic relationship between lipophilicity and biological activity, an optimum partition coefficient is usually identified within each group of homologous analogs.[16] Accordingly, it is possible that more water-soluble candidates, which show moderate improvements in lipophilicities, will demonstrate better transmembrane diffusion than the relatively more hydrophobic aliphatic amides. These permeability and biological activity studies remain to be completed.

The DFO derivatives evaluated in this study form a basis on which alternative modifications may lead to analogs with optimized physicochemical solution properties that lead to improved biomembrane permeabilities. The information gathered from this study suggests that derivatization of the primary amino group of DFO with more bulky, polar, and unsaturated moieties would decrease the melting points and may enhance the ability to establish solute–solvent interactions.

## ACKNOWLEDGMENTS

This research was supported by the American Heart Association (Nebraska Affiliate) and the University of Nebraska Medical Center. P. Ihnat was supported by the American Foundation for Pharmaceutical Education.

## REFERENCES

1. Keberle H. 1964. The biochemistry of desferrioxamine and its relation to iron metabolism. Ann NY Acad Sci 119:758–768.
2. Olivieri NF, Brittenham GM, Matsui D, Berkovitch M, Blendis LM, Cameron RG, McClelland RA, Liu PP, Templeton DM, Koren G. 1995. N Engl J Med 332:918–922.
3. Schnebli HP, Hassan I, Hamilton KO, Lynch S, Jin Y, Nick HP, Peter HH, Junker Walker U, Ziel R, Khanna SC, Dean R, Bergeron RJ. 1994. Toward better chelation therapy: Current concepts and research strategy. In: Bergeron RJ, Brittenham GM, editors. The development of iron chelators for clinical use. Boca Raton, FL: CRC Press, pp 131–147.
4. Lloyd JB, Cable H, Rice-Evans C. 1991. Evidence that desferrioxamine cannot enter cells by passive diffusion. Biochem Pharmacol 41:1361–1363.
5. Basco LK, LeBras J. 1993. *In vitro* activity of chloroquine and quinine in combination with desferrioxamine against *Plasmodium falciparum*. Am J Haematol 42:389–391.
6. Mabeza GF, Loyevsky M, Gordeuk VR, Weiss G. 1999. Iron chelation therapy for malaria. Pharmacol Ther 81:53–75.
7. Halliwell B. 1989. Protection against tissue damage *in vivo* by desferrioxamine: What is its mechanism of action? Free Rad Biol Med 7:645–651.
8. Ihnat PM, Robinson DH. 1993. Potentiometric determination of the thermodynamic ionization constants of deferoxamine. J Pharm Sci 82:110–112.
9. Pitman IH, 1981. Prodrugs of amides, imides and amines. Med Res Rev 1:189–214.
10. Leo A, Hansch C, Elkins D. 1971. Chem Rev 71: 525–616.
11. Ho NFH, Park YJ, Morozowich W, Higuchi WI. 1977. Physical model approach to the design of drugs with improved intestinal absorption. In: Roche EB, editor. Design of biopharmaceutical properties through prodrugs and analogs. Washington, DC:American Pharmaceutical Association, pp 136–227.
12. Smith RN, Hansch C, Ames MM. 1975. Selection of a reference partitioning system for drug design work. J Pharm Sci 64:559–606.
13. Franks NP, Abraham MH, Lieb WR. 1993. Molecular organization of liquid n-octanol: An x-ray diffraction analysis. J Pharm Sci 82:466–470.
14. Diamond JM, Wright EM. 1969. Molecular forces governing nonelectrolyte permeation through cell membranes. Proc Roy Soc B 172:273–316.
15. Yalkowsky SH, Flynn GL, Slunick TG. 1972. J Pharm Sci 61:852–857.
16. Hansch C, Clayton JM. 1973. Lipophilic character and biological activity of drugs II: The parabolic case. J Pharm Sci 62:1–21.
17. Schwarzenbach G, Schwarzenbach K. 1963. Hy-

droxoamtkomplexe I: Die stabilitat der eisen (III)-komplexe einfacher hydroxamsauren und des ferrioxamins B. Helv Chim Acta 46:1390–1400.
18. Rodgers SJ, Raymond KN. 1983. Ferric ion sequestering agents 11: Synthesis and kinetics of iron removal from transferrin of catechoyl derivatives of desferrioxamine B. J Med Chem 26:439–442.
19. Schmidhammer H, Brossi A. 1982. Synthesis of (-)and (+)-2-hydroxy-6-keto-N-methylmorphinans, their O-methyl ethers and 2-deoxy congeners. Can J Chem 60:3055–3060.
20. Monzyk B, Crumbliss AL. 1983. Factors that influence siderophore mediated iron bioavailability: Catalysis of interligand iron (III) transfer from ferrioxamine B to EDTA by hydroxamic acids. J Inorg Biochem 19:19–39.
21. Ihnat PM. 1995. Design and characterization of deferoxamine derivatives with improved biomembrane permeability. Ph.D. Dissertation, University of Nebraska Medical Center, Omaha, Nebraska.
22. Dearden JC, Bresnen GM. 1988. The measurement of partition coefficients. Quant Struct-Act Relat 7: 133–144.
23. Grand DJW, Higuchi T. 1990. In: Solubility behavior of organic compounds. New York: John Wiley & Sons Inc.
24. Stein WD. 1967 In: The movement of molecules across cell membranes. New York: Academic Press.
25. Bauer L, Exner O. 1974. The chemistry of hydroxamic acids and N-hydroxyimides. Angew Chem, Int Ed Engl 13:376–383.
26. Lipczynska-Kochany E, Iwamura H. 1982. Oxygen-17 NMR studies of the structures of benzohydroxamic acids and benzohydroxamate ions in solution. J Org Chem 47:5277–5282.
27. Buckton G, Beezer AE, Denyer SP, Russell SJ. 1991. Observations on the biopharmaceutical importance of chain length in chemically related compounds. Int J Pharm 73:1–7.
28. Forster S, Buckton G, Beezer AE. 1991. The importance of chain length on the wettability and solubility of organic homologs. Int J Pharm 72:29–34.
29. Yalkowsky SH, Valvani SC, Roseman TJ. 1983. Solubility and partitioning IV: Octanol solubility and octanol-water partition coefficients. J Pharm Sci 72:866–870.
30. Schwartz PA, Paruta AN. 1976. Solution thermodynamics of alkyl p-aminobenzoates. J Pharm Sci 65:252–257.
31. Conradi RA, Hilgers AR, Ho NFH, Burton PS. 1991. The influence of peptide structure on transport across Caco-2 cells. Pharm Res 8:1453–1460.